

Article

Impact of the Complementarity between Variable Generation Resources and Load on the Flexibility of the Korean Power System

Chang-Gi Min and Mun-Kyeom Kim *

Department of Energy System Engineering, Chung-Ang University, 84 Heukseok-ro, Dongjak-gu, Seoul 06974, Korea; cgmin@snu.ac.kr

* Correspondence: mkim@cau.ac.kr; Tel.: +82-2-820-5271

Received: 18 September 2017; Accepted: 26 October 2017; Published: 27 October 2017

Abstract: This study examines the effect of the complementarity between the variable generation resources (VGRs) and the load on the flexibility of the power system. The complementarity may change the ramping capability requirement, and thereby, the flexibility. This effect is quantified using a flexibility index called the ramping capability shortage expectation (RSE). The flexibility is evaluated for different VGR mix scenarios under the same VGR penetration level, and an optimal VGR mix (i.e., one that maximizes flexibility) is obtained. The effect of the complementarity of the wind and PV outputs on the flexibility is investigated for the peak-load day of 2016 for the Korean power system. The result shows that the RSE value for the optimal VGR mix scenario is 6.95% larger than that for the original mix scenario.

Keywords: complementarity; flexibility; optimal mix; ramping capability; ramping capability shortage expectation; variable generation resource

1. Introduction

The European Union (EU) has set a target of a 40% reduction in greenhouse gas (GHG) emission from its level in the 1990s, and has agreed to increase the share of renewable energy sources (RES) in energy consumption to 27% by 2030. The Energy Roadmap 2050 has also reported that the share of electricity in the energy system may be almost doubled by 2050, compared to the value in 2011. According to the high renewables scenario, approximately 97% of the electricity consumption would be supplied by RES. Among the RES, variable generation resources (VGRs) share the largest percentage, and their expansion is already progressing rapidly. For example, the share of RES capacity in Denmark and Spain in 2013 was 56% and 42%, respectively, and VGRs, such as wind and PV systems constituted 83% and 59% of this share, respectively [1]. In Korea, according to the national expansion plan [2], the share of VGR is expected to account for approximately 22% of the total installed capacity by 2029.

The major challenge related to the high penetration of VGR is the increased variability and uncertainty, which causes flexibility issues in the power system. Here, the flexibility means the ability to respond to changes in net load, and the flexibility issues (or problems) indicates the situation that the system may have less flexibility [3,4]. The VGRs are the nondispatchable resources, whose power outputs cannot be adjusted by the system operator in the power system. The VGR output is determined by weather conditions; thus, its variability and uncertainty should be followed by the dispatchable resources. The higher the VGR penetration, the harder it is to satisfy the net load, i.e., the load subtracted by the VGR output. To cope with this difficulty of balancing the net load, more dispatchable and flexible resources are required [5–8].

The VGRs have been regarded as causing the flexibility problem, and part of the conventional generators (e.g., gas power generation) are thought to be one of the major flexible resources that

provide flexibility. However, it is worth noting the fact that the VGRs have also been considered a type of flexible resource by virtue of the following two aspects: controllability and complementarity [9,10]. The former relates to technically changing the VGRs into a type of dispatchable resource. The latter is associated with the utilization of the correlation between VGR outputs to improve flexibility. In this study, we focus on the latter aspect.

The complementarity between VGRs in power systems has been receiving attention because it can reduce the VGR variability, thereby helping to secure flexibility. Temporal and regional complementarities between the VGRs have been considered as important aspects that reduce the variability of power systems [11]. However, in relation to the flexibility issue, an important aspect is not the complementarity between VGR outputs, but that between the load and the VGR output. The former does not necessarily mitigate the net load variability and, therefore, may not be helpful in improving the flexibility, while the latter directly relates to the net load variability. For example, when the load increases, increasing the VGR output is better for balancing power than maintaining a constant VGR output flattened by the complementarity. Moreover, a complementarity that is effective in one system may not be effective for another system. The impact may differ with the operating conditions of each system: e.g., the more fast-ramping resources a system has, the more effective it will be in responding to the net load variance. Therefore, the complementarity between the VGR output and load should be evaluated in tandem with the operating conditions.

Various studies have investigated the complementarity [12–27]. These studies have mostly focused on the complementarity between VGR outputs. Most of them have found the flattening effect of aggregated VGR output; for reference, the wind–solar hybrid systems have been the most studied systems [12–20]. A combination of solar and hydro systems, and that combination plus wind or ocean-wave systems, have also been addressed [21–27]. There has also been research on the synergy effect between wind and the solar system, i.e., rather increasing variability [14]. Most of these studies have evaluated the complementarity based on statistical analysis: they have used statistical indices such as the correlation coefficient, standard deviation, mean, etc. These approaches do not consider the operating conditions of the system well and, hence, they do not reflect the generation side, and accordingly, the flexibility. A few other studies have proposed new indices on complementarity [14,18,22]. These new index-based studies have dealt with the complementarity between the VGR output and the load. Among these studies, there has been an effort to investigate the effect of VGR combinations on the flexibility [14]. However, they did not explicitly evaluate the amount of ramping capability (RC) provided by the system against the net load variation; i.e., the operating conditions related to flexibility were neglected.

This study uses the RC shortage expectation (RSE) to quantify the impact of the complementarity between the VGR output and the load, on the flexibility [28]. This index is capable of evaluating the extent to which the uncertainty and variability in the net load is covered by the RC. The complementarities for different VGR mix scenarios are evaluated, i.e., the RSE value for each scenario is calculated. We then find an optimal mix scenario in terms of flexibility. A case study for the peak-load day of 2016 in Korea is conducted, and the flexibility according to the changes in wind and PV ratios is calculated.

The rest of this paper is organized as follows: Section 2 explains the flexibility index RSE, which quantifies the complementarity effect. Section 3 describes a methodology to find the VGR optimal mix. In Section 4, the case study for the peak-load day of 2016 in Korea is described. The conclusion and future works are given in Section 5.

2. Flexibility Index: Ramping Capability Shortage Expectation

Power system operators need to cope with net load variability and uncertainty, which directly relate to the flexibility of the power system. The larger the variability and uncertainty, the more flexibility that is required. The system's ability to react to the increased variability and uncertainty is mainly provided by the RC, which is defined as the ability of a generator to increase/decrease

its power output against load variations in the considered period. Thus, the flexibility is largely affected by the extent to which the system can provide RC. The higher the RC is, the larger the flexibility will be. Meanwhile, the complementarity between the VGR and the load can also be helpful for the flexibility. For example, the VGR perfectly correlates with the load in a different direction, i.e., the increase (decrease) in VGR according to the increase (decrease) in load, can decrease the net load variability in large VGR-integrated systems. The complementarity can reduce the flexibility requirement. The flexibility index RSE can capture not only the RC, but also the net load change with the complementarity [28].

Ramping Capability Shortage Expectation (RSE)

The RC is of great importance as a measure to provide flexibility. Securing more RC helps enhance the flexibility of the power system. However, uncertainties, such as generator failure and net load forecast error in the system, make it more difficult to ensure RC availability. The risk index RSE has been proposed to capture the impact of these uncertainties on the flexibility evaluation. The RSE calculation can be briefly described using the following equations:

The RC requirement (RCR) is expressed as follows:

$$RCR_t = NLFE_t + FNL_t - \sum_{i \in I} A_{i,t-\Delta t} O_{i,t-\Delta t} P_{i,t-\Delta t}, \quad (1)$$

where:

$$NLFE_t = LFE_t - VGFE_t, \quad (2)$$

$$FNL_t = FL_t - FVG_t. \quad (3)$$

RCR_t indicates the amount of RC required when considering the load increase/decrease and the failures of loading generators during the interval from $t - \Delta t$ to t . It should be noted that the RCR_t relates to the “interval” from $t - \Delta t$ to t . Equation (1) includes information not only at $t - \Delta t$, but also at t . $A_{i,t-\Delta t}$, $NLFE_t$, LFE_t , and $VGFE_t$ are random variables; $A_{i,t-\Delta t}$ relates to the generator failure, while the remaining three variables represent the forecast error. The details for the $A_{i,t-\Delta t}$ calculation are provided in [28].

The system RC (SRC) is calculated as the sum of RCs of all generators and is given by:

$$SRC_t = \sum_{i \in I} A_{i,t-\Delta t} O_{i,t-\Delta t} \min(P_{max,i} - P_{i,t-\Delta t}, rr_i \Delta t). \quad (4)$$

The SRC_t indicates the extent to which the system can provide the RC, considering the failure of online generators from $t - \Delta t$ to t . The uncertainty factors are included in both RCR_t and SRC_t . Here, $O_{i,t-\Delta t}$ and $P_{i,t-\Delta t}$ are determined by a generation schedule.

If RCR_t is larger than SRC_t , load shedding occurs: this is called the RC shortage. The RC shortage probability (RSP) is defined as the probability that RC shortage will occur at time t , and is given by:

$$RSP_t = \sum_{e \in E_t} Prob(e) \left[\sum_{c \in C_{t-\Delta t}} Prob_c \left[FNL_t + NLFE_t > \sum_{i \in I} A_{i,t-\Delta t} O_{i,t-\Delta t} \{P_{i,t-\Delta t} + \min(P_{max,i} - P_{i,t-\Delta t}, rr_i \Delta t)\} \right] \right] \quad (5)$$

and the RSE is calculated as follows:

$$RSE = \sum_t RSP_t \quad (6)$$

$C_{t-\Delta t}$ and E_t are the sets representing the uncertainty scenarios for $A_{i,t-\Delta t}$ and $NLFE_t$, respectively. Here, a simple example for finding $C_{t-\Delta t}$ is mentioned: Assume that two generators (G1, G2) are online for a period of two hours, and the interval is 1. C_1 is represented using a combination of the states of G1 and G2, i.e., $(A_{1,1}, A_{2,1})$. Each generator has two states, i.e., 0 (failure) or 1 (online). Thus, C_1 consists of “(0, 0), (0, 1), (1, 0), (1, 1).” The probability of each element is calculated using a Markov-chain-based

two-state model [29]. An example for determining E_t is also provided here: Assume that the forecast net loads (i.e., FNL_t) for hours 1 and 2 are 10 MW and 20 MW, respectively, and its error, i.e., NLFE, follows the triangular distribution shown in Figure 1. E_1 and E_2 can be “(−0.5), (0), (0.5)” and “(−1.0), (0), (1.0),” respectively.

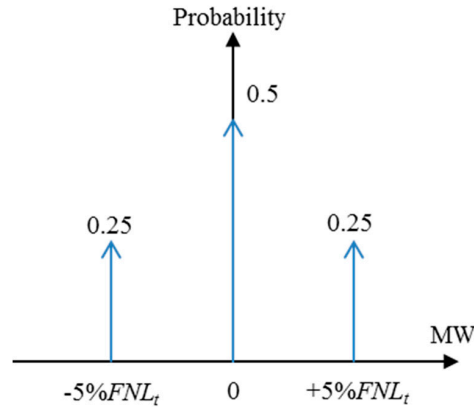


Figure 1. Triangular distribution for the example.

It should be noted that the complementarity effect of the VGR outputs can be reflected by the changes in $NLFE_t$, $VGFE_t$, $O_{i,t-\Delta t}$, and $P_{i,t-\Delta t}$. The changes in the aggregated VGR output changes the value of FVG_t , and accordingly, the $VGFE_t$ and $NLFE_t$. The changes may also alter the operating points of generators; it means that the $O_{i,t-\Delta t}$, and $P_{i,t-\Delta t}$ may vary.

The RSE calculation has the following characteristics: (1) only the risk with regard to increasing the net load is considered; and (2) the worst case in time is applied to the RSE calculation. The second characteristic is very helpful to reduce the computational burden in large power systems.

3. VGR Optimal Mix

A scenario-based approach is used to find the VGR optimal mix for the VGR penetration level in the power system. In this approach, VGR mix scenarios are generated under the same VGR penetration level, and the RSE is calculated for the VGR output for each scenario. The RSE calculation is repeated for every VGR mix scenario to find an optimal VGR mix ratio. However, the optimality is guaranteed only within the considered VGR mix scenarios, i.e., other cases outside the scenarios are not considered. The following steps represent the detailed procedure to generate the VGR mix scenarios and to evaluate the flexibility (i.e., RSE):

- Step 1. Select a peak-load day. The input data related to the RSE calculation and the generation scheduling for a day is required. For reference, the input data for the RSE calculation are as follows: load and VGR output profiles, generator's failure and repair rates, forecast error distributions of the load and VGR output, and generation schedule result.
- Step 2. Select more than two VGRs from among the VGR for the day. For reference, all VGRs, of course, can be selected; however, selecting all VGRs may be inefficient because the share of some VGRs is too small to affect the flexibility.
- Step 3. Find the mix ratio of the selected VGR.
- Step 4. Generate the VGR mix scenarios, i.e., change the ratios in lexicographic order with a constant step size, keeping the same VGR penetration level:

$$VG = \sum_{j=1} \alpha_j VG_j + \alpha_{ns} VG_{ns} \quad (7)$$

where:

$$\sum_{j=1} \alpha_j + \alpha_{ns} = 1 \ \& \ \alpha_j \geq 0 \ \text{for } \forall j \quad (8)$$

An example of Steps 1 to 4 is given next: Assume that the step size is 0.1, and the original ratios of the three VGRs are 0.1, 0.2, and 0.5, respectively. Their sum is 0.8. The ratio of the non-selected VGR is 0.2. The ratio of the first VGR starts from 0 to 1 with a step size of 0.1, i.e., 0, 0.1, ..., 0.9, 1.0. For these changes in the ratio of the first VGR, the ratio of the second VGR is changed from 0 to a maximum value, e.g., if the ratio of the first VGR is 0.3, the possible maximum value of the second VGR is 0.5 when the ratio of the third VGR is 0. Finally, the ratio of the third VGR is determined by the total sum of mix ratios (i.e., 0.8) minus the sum of the ratios of the first and second VGRs. By finding all VGR mix ratios with no overlap, all VGR scenarios can be obtained.

- Step 5. Calculate the RSE value (i.e., flexibility) for every scenario, using Equations (5) and (6). The VGR mix scenario having the smallest RSE value is determined as the optimal VGR mix scenario.

The steps above are summarized as shown in Figure 2.

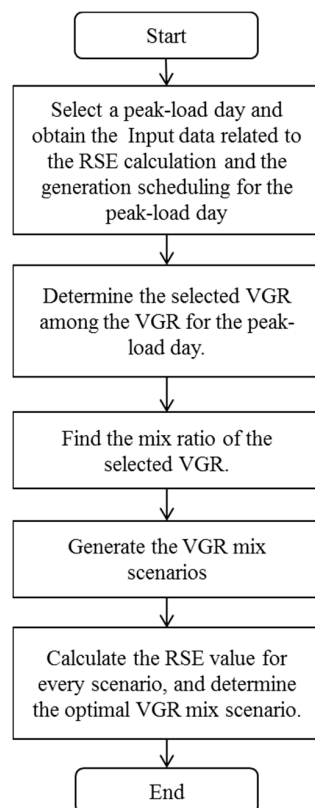


Figure 2. Procedure to find the VGR optimal mix.

4. Case Study

The main objective of this study is to confirm the impact of the changes in the VGR mix ratio on the flexibility of the Korean power system. A market simulation program M-CoreS is used to solve the generation schedule in the Korea electricity market [30]. The RSE is computed using the MATLAB program (R2012b version, MathWorks, Natick, MA, USA) [31]. All simulations are performed on a PC with a 3.70 GHz Intel Core i3-6100 CPU and 16 GB RAM. The peak-load day for 2016 is selected for this simulation [32]. The $VGFE_t$ and $NLFE_t$ are assumed to follow a Gaussian distribution with

a standard deviation of 5%. The information of the generators and their failure and repair rates are present in [8,33], respectively.

The available capacity of the dispatchable units (excluding the maintenance-scheduled and failed units) is 85,216 MW. For simplicity, it is assumed that the reserve capacity of the pumped hydroelectric storage (PHES) units is not available (but its energy production is available). In Korea, both the VGRs and non-VGRs are included among the nondispatchable resources, which are units operated by self-scheduling by their owners. The non-VGRs contain the following types of resources: biofuel, fuel cell, waste power, etc. The sum of the available capacity of the nondispatchable units in a day is 4104 MW. The installed capacity of the wind and PV systems constitutes approximately 63.0% of the installed capacity of the nondispatchable units and 94.7% of the VGRs. Thus, the wind and PV systems are selected to generate the VGR mix scenarios. The penetration level of the selected VGRs is 3.4%. Figure 3 shows the output profiles of the selected VGRs and non-VGRs. The output profiles of the selected VGRs (i.e., wind and PV systems) for the peak-load day are shown in Figure 4 [32].

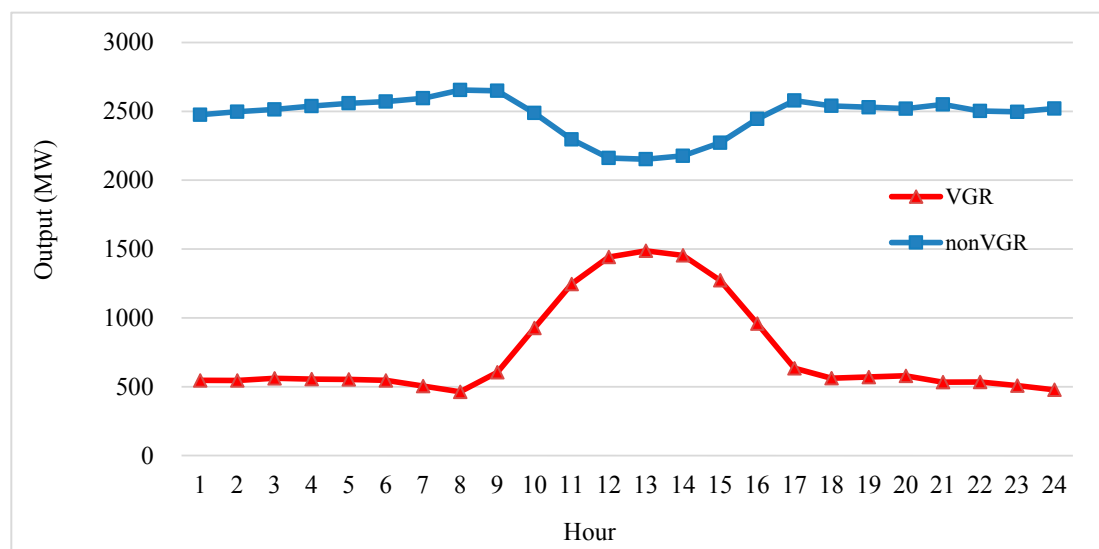


Figure 3. Output profiles of the selected VGRs (i.e., wind and PV systems) and non-VGRs for the peak-load day.

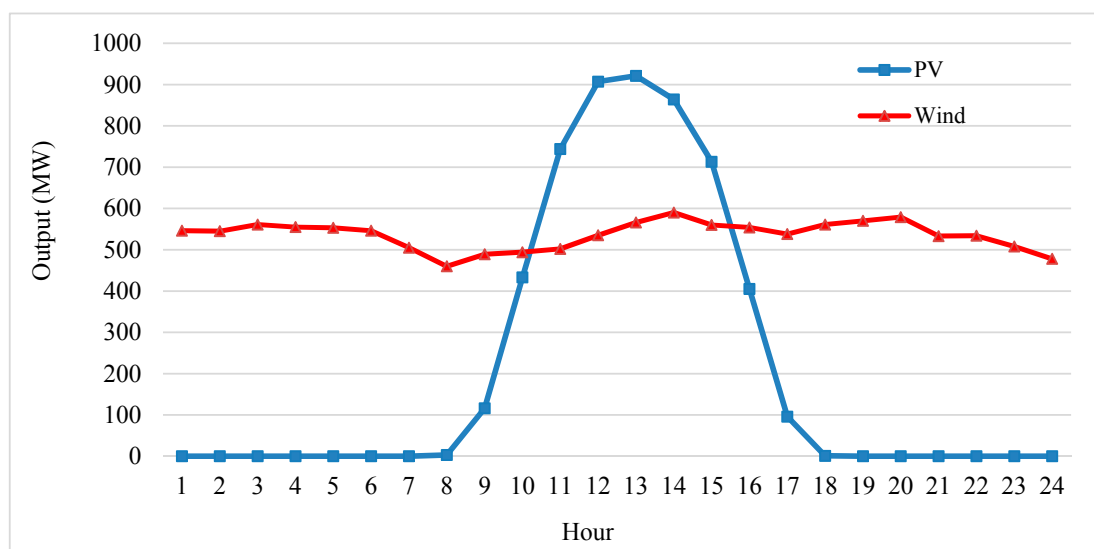


Figure 4. Output profiles of the selected VGRs (i.e., wind and PV systems) for the peak-load day.

The installed capacities of the wind and PV systems are 1047 MW and 1.37 MW, respectively. The ratios of the wind and PV systems to the total VGRs are 56.3% and 38.4%, respectively; and that of the remaining VGRs to the total VGRs is 5.3%. The ratio of the selected VGRs is changed with a step size of 5% under the same VGR penetration level, while the ratio of the nonselected VGRs is fixed. The VGR mix scenarios are given in Table 1. The original VGR mix scenario corresponds to S12. Figures 5 and 6 show the output profiles of the PV and wind systems, respectively, according to the VGR mix scenarios. Figure 7 shows the aggregated output profile of the selected VGR. The difference between the minimum and maximum values of the output of the selected VGR increases as the wind (PV) ratio decreases (increases). This mainly originates from the output profile of the PV system.

Table 1. VGR mix scenarios for the peak-load day.

Scenario	PV Ratio [%]	Wind Ratio [%]
S1	1.3	93.4
S2	6.3	88.4
S3	11.3	83.4
S4	16.3	78.4
S5	21.3	73.4
S6	26.3	68.4
S7	31.3	63.4
S8	36.3	58.4
S9	41.3	53.4
S10	46.3	48.4
S11	51.3	43.4
S12	56.3	38.4
S13	61.3	33.4
S14	66.3	28.4
S15	71.3	23.4
S16	76.3	18.4
S17	81.3	13.4
S18	86.3	8.4
S19	91.3	3.4

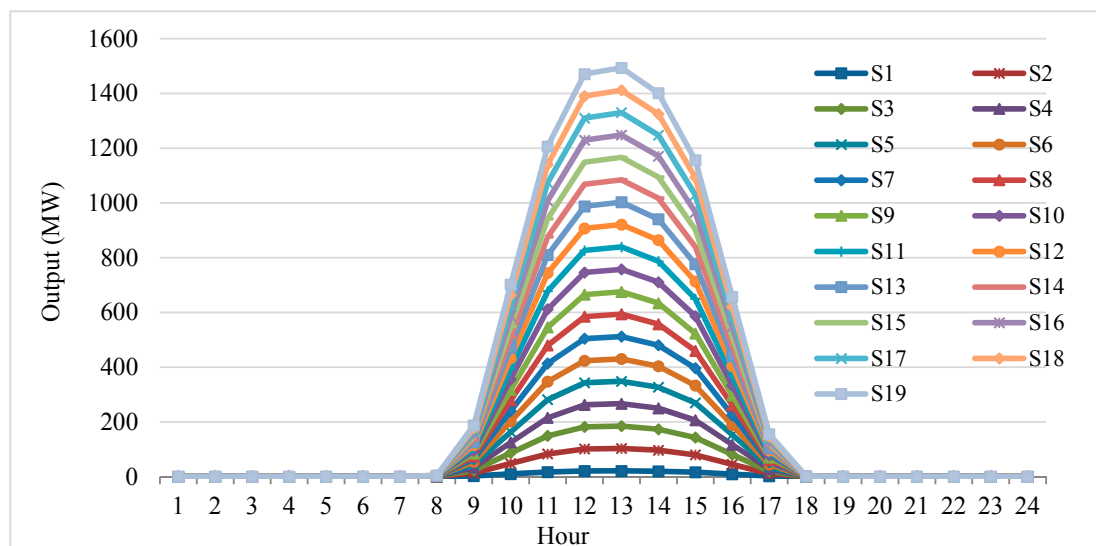


Figure 5. Output profile of PV according to the VGR mix scenarios.

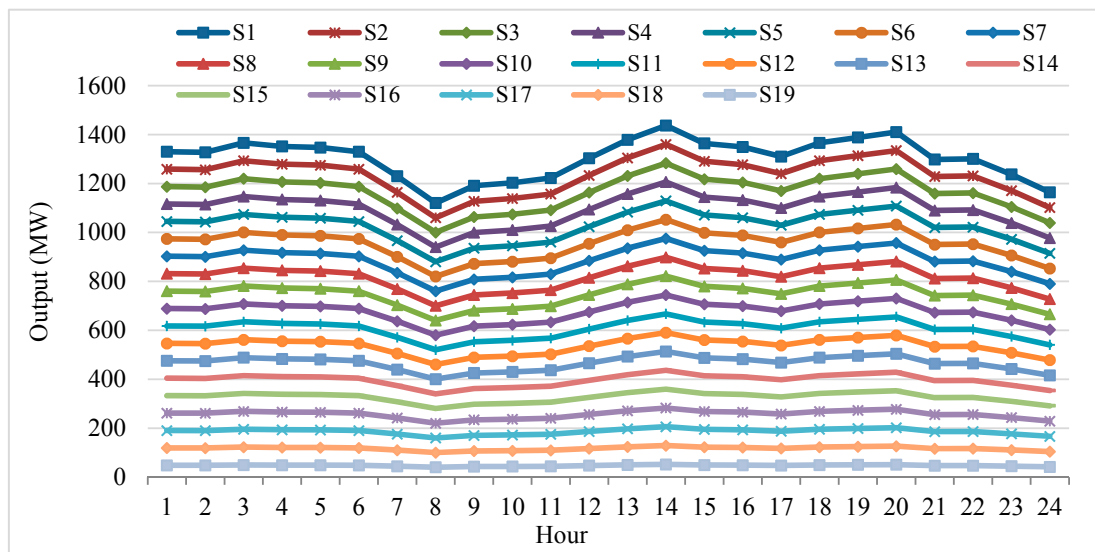


Figure 6. Output profile of the wind system according to the VGR mix scenarios.

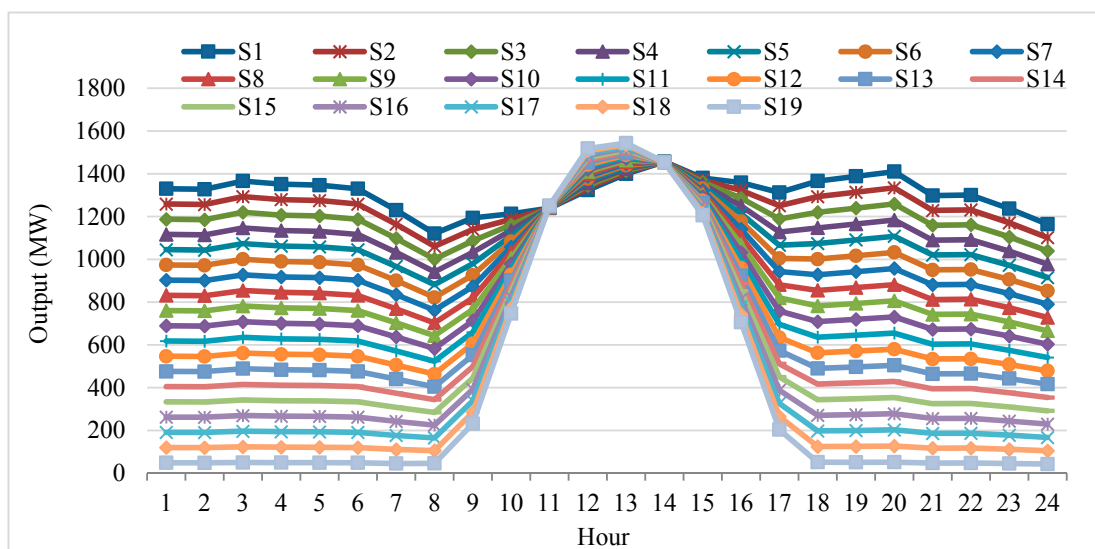


Figure 7. Output profile of the selected VGR for the peak-load day.

Using the output profiles given above, the net load profile is obtained as shown in Figure 8; the complementarity effect is reflected in the net load profile of each VGR mix scenario. S1 (S19) is the most wind (PV)-oriented VGR mix scenario. Figures 9 and 10 show the results for the generation schedules for S1 and S19, respectively. Table 2 lists the RSE values for every VGR mix scenario. S1 results in the lowest RSE value, i.e., 9.9435 (hours/day). It is an optimal VGR mix scenario; the ratios of wind and PV to the total VGR are 93.4% and 1.3%, respectively. The RSE value of S1 is 6.95% larger than that of the original VGR mix scenario (i.e., S12). Meanwhile, S16 makes the largest RSE. The difference between the RSE values of S1 and S16 is due to the difference between the net load profiles of the VGR mix scenarios. The RSP values for S1 and S16 are compared in Figure 11, for further details. A tendency wherein the RSE increases as the PV (wind) ratio increases (decreases) is found, although it is not evident all the time. This may because the wind system has a larger capacity factor and a smaller variability; the capacity factors of the wind and PV systems are 14.1% and 34.9%, respectively [32].

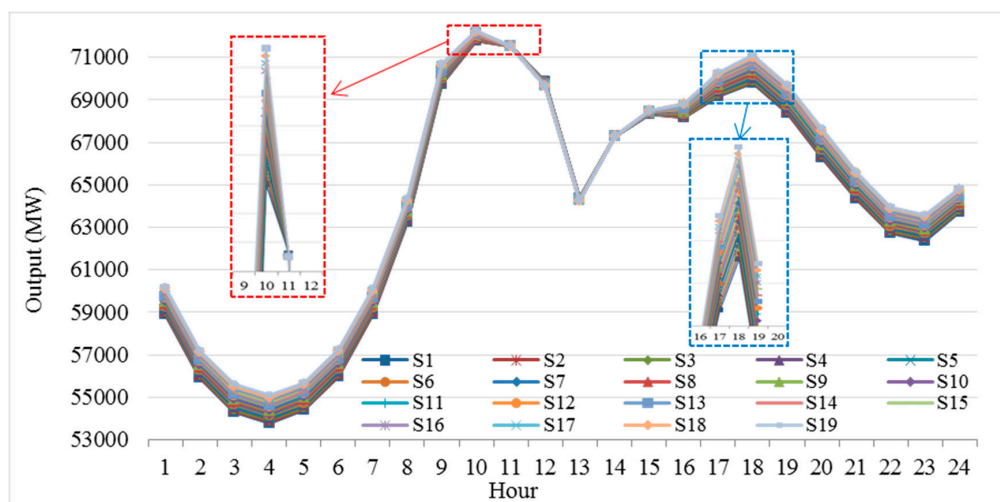


Figure 8. Net load profile for the VGR mix scenario.

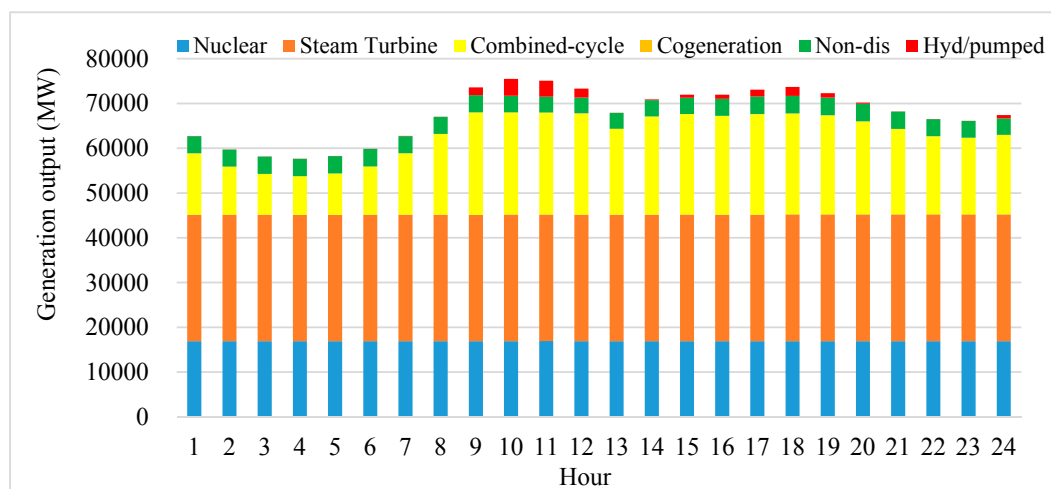


Figure 9. Generation schedule result for S1.

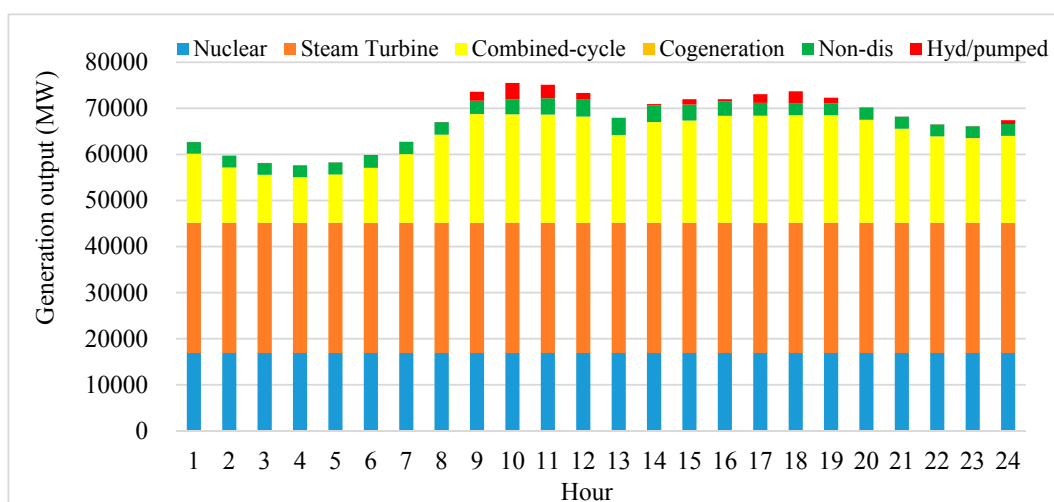
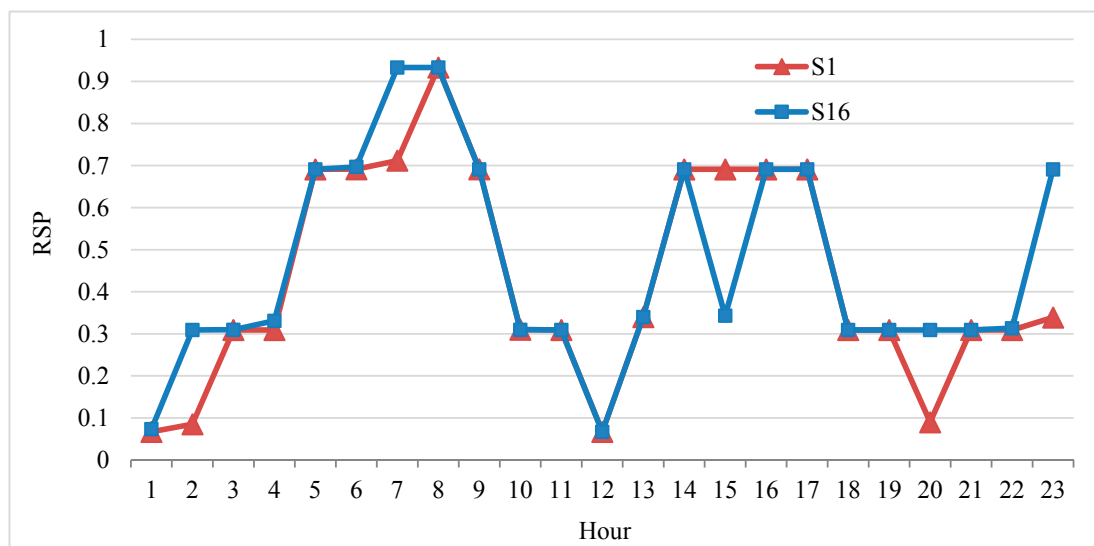


Figure 10. Generation schedule result for S19.

Table 2. RSE values for VGR mix scenarios.

Scenario	RSE [hours/day]
S1	9.9435
S2	10.6189
S3	10.2710
S4	10.6162
S5	10.6172
S6	10.5893
S7	10.3990
S8	10.6027
S9	10.6156
S10	10.6136
S11	10.6273
S12	10.6346
S13	10.6370
S14	10.6192
S15	10.6417
S16	10.6500
S17	10.6106
S18	10.5961
S19	10.6263

**Figure 11.** RSP value for S1 and S16.

5. Conclusions

This study investigated the impact of the complementarity between the VGR and the load on the flexibility in Korean power systems. The effect of the complementarity between the VGR and load was captured using a flexibility index named the RC shortage expectation (RSE). The peak-load day of 2016 in Korea was used in this study. We examined an optimal mix ratio between the wind and PV systems using the VGR mix scenarios; the ratios of the wind and PV systems to the total VGR were 1.3% and 93.4%, respectively. These results may provide useful information for the system operator to secure flexibility in large VGR-integrated systems. As part of future works, we plan to examine the impact of the complementarity between the PHES and the VGR on the flexibility. It would also be interesting to study the effect of the location and model of the load and variable generation resources on the flexibility.

Acknowledgments: This research was supported by the Korea Electric Power Corporation through the Korea Electrical Engineering and Science Research Institute (grant number: R15XA03-55) and Basic Science Research Program through the National Research Foundation of Korea (NRF) funded by the Ministry of Education (2017R1D1A1B03029308).

Author Contributions: Chang-Gi Min conducted most of the research and Mun-Kyeom Kim reviewed the work continuously.

Conflicts of Interest: The authors declare no conflicts of interest.

Nomenclature

$A_{i,t}$	Random variable representing availability of generator i at time t (1 if available, 0 otherwise)
α_{ns}	Ratio of non-selected VGR j to total VGR
α_j	Ratio of selected VGR j to total VGR
c	Element of $C_{t-\Delta t}$
$C_{t-\Delta t}$	Set of combinations of $A_{i,t-\Delta t}$ when $O_{i,t-\Delta t}$ is nonzero for all i
e	Element of E_t
E_t	Set of $NLFE_t$
FL_t	Forecast load at time t
FNL_t	Forecast net load at time t
FVG_t	Forecast variable generation at time t
i	Index of generator
I	Set of generators
j	Index of VGR
LFE_t	Random variable representing load forecast error at time t
$NLFE_t$	Random variable representing net load forecast error at time t
$O_{i,t}$	Value representing whether generator i is online at time t or not
$P_{i,t}$	Output of generator i at time t
$P_{\max,i}$	Maximum output level of generator i
PHES	Pumped hydroelectric storage
$Prob(\cdot)$	Probability in the brackets.
$Prob_c[\cdot]$	Probability of c if condition $[\cdot]$ is satisfied, 0 otherwise.
RCR_t	Ramping capability requirement at time t
rr_i	Ramp rate of generator i
RES	Renewable energy sources
RSP_t	Ramping capability shortage probability at time t
SRC_t	System ramping capability at time t
t	Index of time
Δt	Minimum interval between operating points
VG	Installed capacity of all VGR
VG_j	Installed capacity of selected VGR j
VG_{ns}	Installed capacity of all nonselected VGRs
VGR	Variable generation resource
$VGFE_t$	Random variable representing variable generation forecast error at time t

References

1. Graabak, I.; Korpås, M. Variability characteristics of european wind and solar power resources—A review. *Energies* **2016**, *9*, 449. [[CrossRef](#)]
2. The Ministry of Trade, Industry and Energy. *The 7th Basic Plan on Electricity Demand and Supply*; MOTIE: Sejong-si, Korea, 2015.
3. Min, C.-G.; Kim, M.-K. Net load carrying capability of generating units in power systems. *Energies* **2017**, *10*, 1221. [[CrossRef](#)]
4. Min, C.-G.; Kim, M.-K. Flexibility-based reserve scheduling of pumped hydroelectric energy storage in Korea. *Energies* **2017**, *10*, 1478.

5. Gabash, A.; Li, P. Active-reactive optimal power flow in distribution networks with embedded generation and battery storage. *IEEE Trans. Power Syst.* **2012**, *27*, 2026–2035. [[CrossRef](#)]
6. Gabash, A.; Li, P. Flexible optimal operation of battery storage systems for energy supply networks. *IEEE Trans. Power Syst.* **2013**, *28*, 2788–2797. [[CrossRef](#)]
7. Gabash, A.; Li, P. On variable reverse power flow-part i: Active-reactive optimal power flow with reactive power of wind stations. *Energies* **2016**, *9*, 121. [[CrossRef](#)]
8. Gabash, A.; Li, P. On variable reverse power flow-part ii: An electricity market model considering wind station size and location. *Energies* **2016**, *9*, 235. [[CrossRef](#)]
9. Díaz-González, F.; Hau, M.; Sumper, A.; Gomis-Bellmunt, O. Participation of wind power plants in system frequency control: Review of grid code requirements and control methods. *Renew. Sustain. Energy Rev.* **2014**, *34*, 551–564. [[CrossRef](#)]
10. Widén, J.; Carpmann, N.; Castellucci, V.; Lingfors, D.; Olauson, J.; Remouit, F.; Bergkvist, M.; Grabbe, M.; Waters, R. Variability assessment and forecasting of renewables: A review for solar, wind, wave and tidal resources. *Renew. Sustain. Energy Rev.* **2015**, *44*, 356–375. [[CrossRef](#)]
11. Xiao, L.; Lin, L.; Liu, Y. Discussions on the architecture and operation mode of future power grids. *Energies* **2011**, *4*, 1025–1035. [[CrossRef](#)]
12. Solomon, A.A.; Faiman, D.; Meron, G. Grid matching of large-scale wind energy conversion systems, alone and in tandem with large-scale photovoltaic systems: An Israeli case study. *Energy Policy* **2010**, *38*, 7070–7081. [[CrossRef](#)]
13. Halamay, D.A.; Brekken, T.K.; Simmons, A.; McArthur, S. Reserve requirement impacts of large-scale integration of wind, solar, and ocean wave power generation. *IEEE Trans. Sustain. Energy* **2011**, *2*, 321–328. [[CrossRef](#)]
14. Prasad, A.A.; Taylor, R.A.; Kay, M. Assessment of solar and wind resource synergy in Australia. *Appl. Energy* **2017**, *190*, 354–367. [[CrossRef](#)]
15. Bett, P.E.; Thornton, H.E. The climatological relationships between wind and solar energy supply in Britain. *Renew. Energy* **2016**, *87*, 96–110. [[CrossRef](#)]
16. Huang, Q.; Shi, Y.; Wang, Y.; Lu, L.; Cui, Y. Multi-turbine wind-solar hybrid system. *Renew. Energy* **2015**, *76*, 401–407. [[CrossRef](#)]
17. Solomon, A.; Kammen, D.M.; Callaway, D. Investigating the impact of wind-solar complementarities on energy storage requirement and the corresponding supply reliability criteria. *Appl. Energy* **2016**, *168*, 130–145. [[CrossRef](#)]
18. Hoicka, C.E.; Rowlands, I.H. Solar and wind resource complementarity: Advancing options for renewable electricity integration in Ontario, Canada. *Renew. Energy* **2011**, *36*, 97–107. [[CrossRef](#)]
19. Huva, R.; Dargaville, R.; Caine, S. Prototype large-scale renewable energy system optimisation for Victoria, Australia. *Energy* **2012**, *41*, 326–334. [[CrossRef](#)]
20. Jerez, S.; Trigo, R.; Sarsa, A.; Lorente-Plazas, R.; Pozo-Vázquez, D.; Montávez, J. Spatio-temporal complementarity between solar and wind power in the Iberian Peninsula. *Energy Procedia* **2013**, *40*, 48–57. [[CrossRef](#)]
21. Patsialis, T.; Kougias, I.; Kazakis, N.; Theodossiou, N.; Droege, P. Supporting renewables' penetration in remote areas through the transformation of non-powered dams. *Energies* **2016**, *9*, 1054. [[CrossRef](#)]
22. Beluco, A.; de Souza, P.K.; Krenzinger, A. A dimensionless index evaluating the time complementarity between solar and hydraulic energies. *Renew. Energy* **2008**, *33*, 2157–2165. [[CrossRef](#)]
23. Kougias, I.; Szabó, S.; Monforti-Ferrario, F.; Huld, T.; Bódis, K. A methodology for optimization of the complementarity between small-hydropower plants and solar pv systems. *Renew. Energy* **2016**, *87*, 1023–1030. [[CrossRef](#)]
24. Fang, W.; Huang, Q.; Huang, S.; Yang, J.; Meng, E.; Li, Y. Optimal sizing of utility-scale photovoltaic power generation complementarily operating with hydropower: A case study of the world's largest hydro-photovoltaic plant. *Energy Convers. Manag.* **2017**, *136*, 161–172. [[CrossRef](#)]
25. Schmidt, J.; Cancelli, R.; Pereira, A.O. An optimal mix of solar pv, wind and hydro power for a low-carbon electricity supply in Brazil. *Renew. Energy* **2016**, *85*, 137–147. [[CrossRef](#)]
26. Beluco, A.; de Souza, P.K.; Krenzinger, A. A method to evaluate the effect of complementarity in time between hydro and solar energy on the performance of hybrid hydro pv generating plants. *Renew. Energy* **2012**, *45*, 24–30. [[CrossRef](#)]

27. Francois, B.; Borga, M.; Creutin, J.-D.; Hingray, B.; Raynaud, D.; Sauterleute, J.-F. Complementarity between solar and hydro power: Sensitivity study to climate characteristics in northern-Italy. *Renew. Energy* **2016**, *86*, 543–553. [[CrossRef](#)]
28. Min, C.-G.; Park, J.K.; Hur, D.; Kim, M.-K. A risk evaluation method for ramping capability shortage in power systems. *Energy* **2016**, *113*, 1316–1324. [[CrossRef](#)]
29. Borges, C.L.T. An overview of reliability models and methods for distribution systems with renewable energy distributed generation. *Renew. Sustain. Energy Rev.* **2012**, *16*, 4008–4015. [[CrossRef](#)]
30. Master's Space. *M-Core User's Manual*; MS: Anyang-si, Korea, 2016.
31. Li, L. *Matlab User Manual*; Matlab: Natick, MA, USA, 2001.
32. Korea Power Exchange. Electric Power Statistics Information System. Available online: <http://epsis.kpx.or.kr/epsis/ekesStaticMain.do?cmd=001001&flag=&locale=EN> (accessed on 8 September 2017).
33. Allan, R.N. *Reliability Evaluation of Power Systems*; Springer Science & Business Media: Berlin, Germany, 2013.



© 2017 by the authors. Licensee MDPI, Basel, Switzerland. This article is an open access article distributed under the terms and conditions of the Creative Commons Attribution (CC BY) license (<http://creativecommons.org/licenses/by/4.0/>).